Synthesis and seawater desalination of molecular sieving zeolitic imidazolate framework membranes

Yaqiong Zhu [a], Krishna M. Gupta [b], Qian Liu [a], Jianwen Jiang [b], Jürgen Caro [c], Aisheng Huang [a,*]

[a] Institute of New Energy Technology, Ningbo Institute of Materials Technology and Engineering, CAS, 1219 Zhongguan Road, 315201 Ningbo, PR China
[b] Department of Chemical and Biomolecular Engineering, National University of Singapore, 117576, Singapore
[c] Institute of Physical Chemistry and Electrochemistry, Leibniz University Hannover, Callinstraße 3-3A, D-30167 Hannover, Germany

HIGHLIGHTS

- Dense ZIF membranes are prepared through bio-inspired polydopamine modification.
- ZIF membranes are developed for the first time for seawater desalination.
- The ZIF membranes show high water flux and ion rejection for seawater desalination.

GRAPHICAL ABSTRACT

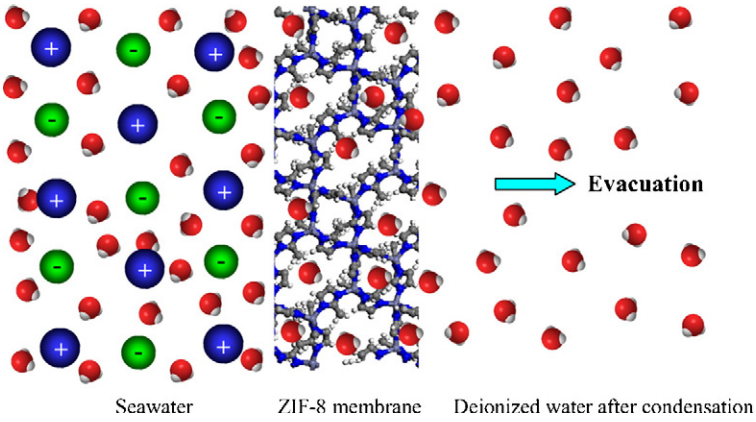

ABSTRACT

Through bio-inspired polydopamine modification of the ceramic support surface, dense and reproducible zeolitic imidazolate framework (ZIF) membranes have been developed for the first time for seawater desalination by pervaporation. Demonstrated by both experimental and simulation studies, the developed ZIF membranes show high desalination performances attributing to the small pore size of the ZIF membranes, which is exactly in between the size of water molecules and hydrated ions. The ZIF membranes show a high stability in seawater. At 25, 50, 75 and 100 °C, the water fluxes through the ZIF-8 membrane are 5.8, 8.1, 10.8, and 13.5 kg/(m^2·h), respectively, with a high ion rejection of over 99.8%, which is promising for seawater desalination by ionic sieving.

Keywords:
Metal–organic frameworks
Zeolitic imidazolate framework
Seawater desalination
Covalent functionalization

1. Introduction

Water scarcity has increasingly become a global challenge to human activities, industrial and agricultural development due to the shortage of freshwater [1]. Therefore, the development of renewable freshwater resources such as seawater desalination plays an important role in resolving the future water supply. Indeed, seawater desalination is expected to offer an unlimited and steady supply of high-quality water without impairing natural freshwater ecosystems [2–4]. In the past half century, many technologies such as multistage flash distillation (MSFD) and reverse osmosis (RO), have been developed for seawater desalination [5]. Comparing with the thermally-based MSFD, the membrane-based RO is considered to be the most promising alternative

* Corresponding author.
E-mail address: huangaisheng@nimte.ac.cn (A. Huang).

because of its low energy consumption [6,7]. However, the present polymeric RO membranes often suffer from biofouling, oxidation, metal oxide fouling, abrasion and mineral scaling, thus usually resulting in a low rejection and low stability [8,9]. Inorganic membranes are expected to break through these material-based limitations for desalination due to their uniform pore structure and high thermal and chemical stability [10–20]. Especially, zeolite MFI (Mobil Five) membranes, including Al-free silicalite-1 and its Al-containing analog ZSM-5 (Zeolite Socony Mobil Five), have been widely examined for desalination [10–14]. However, it should be noted that the thermal burning of organic templates used in the synthesis of zeolite MFI membranes may result in the formation of cracks [21,22], leading to poor reproducibility of membrane preparation. It is highly desired, therefore, to develop novel molecular sieving membranes that can be facilely prepared and activated, and thus effectively used for seawater desalination.

Since no templates/structure directing agents (SDAs) are used in the synthesis of metal–organic frameworks (MOFs) membranes, they can be easier activated than zeolite membranes, and the occluded solvent molecules can be easily removed under mild conditions (e.g. vacuum or heating with activation temperatures below 150 °C). Further, MOFs can better stand thermal expansions/shrinking of the supports upon heating/cooling cycles in comparison with zeolites. Therefore, recently, MOFs have emerged as a novel type of microporous materials for the fabrication of molecular sieve membranes [23–26]. Among the reported MOF membranes, zeolitic imidazolate framework (ZIF) membranes, based on the assembly of transition metals (Zn, Co) and imidazolates [27], have attracted intense interest due to their exceptionally thermal and chemical stability [28]. In the past five years, a series of ZIF membranes have been prepared for gas separation [29–40]. To the best of our knowledge, however, no studies on ZIF membranes have been reported for seawater desalination.

Pervaporation has been widely studied for the separation of organics/water mixtures due to its low energy consumption and ease of operation. Recently, pervaporation is also recommended to be a promising technique for seawater desalination due to its low energy consumption and ease of operation [13,16,17]. In the present work, we make the first attempt to evaluate molecular sieve ZIF-8 (one of the most promising MOF structures because of its outstanding thermal and hydrothermal stability) membranes for seawater desalination by pervaporation. ZIF-8 shows a permanent microporosity with narrow pores size (about 0.34 nm) [27], which is just between the size of water molecules (0.26 nm) and hydrated ions (e.g. Na^+ 0.72 nm, K^+ 0.66 nm, Ca^{2+} 0.82 nm, Mg^{2+} 0.86 nm, Cl^- 0.66 nm, Table 1). Therefore, it can be expected that ZIF-8 membranes could show high water flux and high salt rejection in seawater desalination because of ionic sieving (Fig. S1).

2. Experimental

2.1. Materials

Chemicals were used as received: Zinc chloride (>98%, Aladdin), zinc nitrate tetrahydrate (>99%, Merck), 2-methylimidazole (>99%, Aladdin), imidazolate-2-carboxyaldehyde (ICA, >97%, Alfa Aesar), benzimidazole (98.5%, Aladdin), sodium formate (>99%, Aladdin), methanol (99.5%, Aladdin), N, N-dimethylformamide (DMF, ≥99.9%, Aladdin), dopamine (DPA, 98%, Aladdin), tris(hydroxymethyl) aminomethane (Tris–HCl, 99%, Aladdin). Porous α-Al_2O_3 disks (Fraunhofer IKTS, Inocermic GmbH, Hermsdorf, Germany: 18 mm in diameter, 1.0 mm in thickness, 70 nm particles in the top layer) were used as supports.

2.2. Dopamine modification of the support surface

Dopamine (2 mg/mL) was dissolved in 10 mM Tris–HCl (pH: 8.5) in an open watch glass (diameter: 180 mm). Then the top surface of the porous α-Al_2O_3 disks was treated with dopamine at 20 °C for 20 h, leading to a polydopamine (PDA) layer deposited on the support surface [32]. After drying, the PDA-modified α-Al_2O_3 supports showed a N_2 permeance similar to non-modified α-Al_2O_3 supports, indicating that PDA modification has no discernibly negative effect on the gas permeance of the support.

Table 1
Ion concentrations in the feed and permeate as well as ion rejections of the ZIF-8 membrane for the main ions in seawater.

Ions	Hydrated diameter (nm)[a]	Ion concentration in feed (ppm)[b]	Ion concentration in permeate (ppm)[b]	Rejection (%)
Na^+	0.72	9032	31	99.7
K^+	0.66	661	1.4	99.8
Ca^{2+}	0.82	247	1.1	99.6
Mg^{2+}	0.86	1267	1.5	99.9
Sr^{2+}	0.62	0.5	0.02	96.0
Cl^-	0.66	13,670	10	99.9
Br^-	0.66	2	0.07	96.5
SO_4^{2-}	1.00	1850	8.6	99.5

[a] Hydrated diameters are adopted from Volkov, A.G.; Paula, S.; Deamer, D. W. Bioelectrochem.Bioenergetics 42 (1997) 153.
[b] The concentrations of cations (Na^+, K^+, Ca^{2+}, Mg^{2+}, Sr^{2+}) in the feed and permeate were analyzed by inductively coupled plasma optical emission spectrometer (ICP-OES). The concentrations of anions (Cl^-, Br^-, SO_4^{2-}) in the feed and permeate were analyzed by ion chromatography.

2.3. Synthesis of ZIF membranes on PDA-modified α-Al_2O_3 disks

ZIF-8 membrane was prepared according to the procedure reported elsewhere [32]. A solid mixture of 0.538 g zinc chloride, 0.648 g 2-methylimidazole and 0.268 g sodium formate was dissolved in 50 ml methanol by ultra sonic treatment. The PDA-modified α-Al_2O_3 disks were placed horizontally facing up in a Teflon autoclave, which was filled with synthesis solution, and heated at 85 °C in air oven for 24 h. After solvothermal reaction and cooling to room temperature, the ZIF-8 membrane was washed with methanol several times to remove the loose powder on the support surface, and then dried in air at room temperature over night for characterization and measurement of seawater desalination.

ZIF-90 membrane was prepared according to the following procedure. Initially, 0.4032 g zinc chloride was dissolved in 30 ml methanol; meanwhile, a solid mixture of 1.1372 g imidazolate-2-carboxyaldehyde and 0.8049 g sodium formate was dissolved in another 30 ml methanol. After stirring about 1 h, the two solutions were mixed and subject to intensive stirring until producing a clear and homogenous solution. The PDA-modified α-Al_2O_3 disks were placed in a Teflon autoclave filled with synthesis solution. Afterwards, the Teflon autoclave was heated to 105 °C in a microwave oven (ETHOS One, MLS) with a temperature-increasing rate of 10 °C min^{-1}, and then synthesis temperature was kept unchanged for 3.5 h. After cooling at a rate of 10 °C min^{-1} to room temperature, the membrane was washed with methanol and dried at room temperature for characterization and measurement of seawater desalination.

ZIF-7 membrane was prepared according to the following procedure. Initially, 2.295 g zinc nitrate tetrahydrate was dissolved in 30 ml DMF; meanwhile, a solid mixture of 1.215 g benzimidazole and 0.0075 g sodium formate was dissolved in another 30 ml DMF. After stirring about 30 min, the two solutions were mixed and subject to intensive stirring until producing a clear and homogenous solution. The PDA-modified α-Al_2O_3 disks were placed in a Teflon autoclave filled with synthesis solution. Afterwards, the Teflon autoclave was heated to 105 °C in a microwave oven (ETHOS One, MLS) with a temperature-increasing rate of 10 °C min^{-1}, and then synthesis temperature was kept unchanged for 3.5 h. After cooling at a rate of 10 °C min^{-1} to room temperature, the membrane was washed with methanol and dried at room temperature for characterization and measurement of seawater desalination.

2.4. Characterizations of ZIF membrane

The morphology and thickness of the ZIF membranes were characterized by field emission scanning electron microscopy (FESEM). FESEM micrographs were taken on an S-4800 (Hitachi) with a cold field emission gun operated at 4 kV and 10 μA. The phase purity and crystallinity of the ZIF membrane was confirmed by X-ray diffraction (XRD). The XRD patterns were recorded at ambient conditions with Bruker D8 ADVANCE X-ray diffractometer with CuKa radiation at 40 kV and 40 mA. After the measurement of seawater desalination, the surface chemical compositions of the ZIF-8 membrane were analyzed by energy-dispersive X-ray spectroscopy (EDXS) using the same FESEM microscope at 20 kV and 20 μA and X-ray photoelectron spectroscopy (XPS, Axis Ultra DLD, Kratos) with a Al Kα line as an X-ray source.

2.5. Seawater desalination measurement through ZIF membranes by pervaporation

Seawater was prepared by dissolving a specified amount of sea salts into deionized water to achieve a concentration of 2–10 wt.%. The ion concentration in seawater was listed in Table 1. The supported ZIF membranes were sealed in a permeation module with silicone O-rings (Fig. S2), and seawater was preheated to 25–100 °C and fed to the membrane side. The whole membrane module was heated in a thermostatic water bath together with the feed solution. The permeate side of the membrane was evacuated with a vacuum pump. Two freezing traps with liquid N_2 cooling were used to collect the permeate at every time interval. The water flux has been determined by the amount of water collected in the two cooling traps. For the determination of ion rejection, the permeate side of the membrane (i.e. the support side, since the ZIF layer was facing the feed sea water) was washed periodically after certain times with de-ionized water to collect possibly permeated salts which have been deposited as crystals on top or inside the porous supporting alumina [13].

The performance of seawater desalination was assessed in terms of permeate flux (J) and total ion rejection (R_i). The permeate flux, F (kg/m^2·h), was calculated by

$$F = \frac{W}{\Delta t \cdot A} \tag{1}$$

where W is the permeate mass (kg), Δt is collecting time (h), A is the membrane area (m^2).

The total ion rejection was defined as the ratio of the ion conductivity in the permeate to that in the feed, and given by

$$R_i = \frac{S_{if} - S_{ip}}{S_{if}} \times 100 \tag{2}$$

where S_{if} and S_{iP} are the ion conductivities in the feed and permeate, respectively. Both S_{if} and S_{iP} were analyzed after water dilution by 100 times. The ions conductivities of the feed and the permeate were measured by conductivity meter (DDSJ-308A, Shanghai REX Instrument Factory).

The ion rejection for every ion was defined as the ratio of the ion concentration in the permeate to that in the feed, and given by

$$R_i = \frac{C_{if} - C_{ip}}{C_{if}} \times 100 \tag{3}$$

where C_{if} and C_{iP} are the ion concentration in the feed and permeate, respectively. Both C_{if} and C_{iP} were analyzed after water dilution by 100 times. The concentrations of cations (Na^+, K^+, Ca^{2+}, Mg^{2+}) in the feed and the permeate were analyzed by inductively coupled plasma optical emission spectrometer (ICP-OES, Optima 7300DV, Perkin Elmer Corporation, USA) with source settings 1130 W RF power. The concentrations of anions (Cl^-, Br^- and SO_4^{2-}) in the feed and the permeate were analyzed by ion chromatography (Dionex Corporation, USA) with an AS-19 column and ASRS 4 mm suppressor.

2.6. Simulation models and methods

To provide microscopic insights into water desalination through the ZIF-8 membrane, molecular simulation was conducted. As illustrated in Figure S3, two chambers were separated by the ZIF-8 membrane with a thickness of 58.86 Å. The atomic coordinates of ZIF-8 were adopted from the experimentally determined X-ray crystallographic data [27]. An aqueous NaCl solution and a vacuum were in the left and right chambers of the membrane, respectively. A graphene plate was in the left chamber to prevent water moving from the right to the left, and it was exerted under a hydraulic pressure. The interactions of the ZIF-8 atoms were described by Lennard-Jones (LJ) and electrostatic potentials. The LJ parameters were taken from the universal force field [41], while the charges of framework atoms were adopted from our previous work [42]. Water, Na^+ and Cl^+ ions were represented by the TIP3P model [43] and the Amber force field [44], respectively. The carbon atoms in graphene plate were mimicked by the LJ potential with parameters as used for carbon nanotubes [45].

Initially, the system was subject to energy minimization using the steepest descent method with a maximum step size of 0.1 Å and a force tolerance of 1 kJ mol^{-1} [27]. Then velocities were assigned according to the Maxwell–Boltzmann distribution at 75 °C. Thereafter, molecular dynamics (MD) simulation was carried out. The periodic boundary conditions were applied in the x and y directions, and the graphene plate could self-adjust its position under a hydraulic pressure. The framework atoms were considered to be rigid, and the SETTLE algorithm [46], was used to maintain the geometry of water. Temperature was controlled by the velocity-rescaled Berendsen thermostat with a relaxation time of 0.1 ps [47]. The LJ interactions were evaluated with a cutoff of 14 Å and the Coulombic interactions were calculated using the particle-mesh Ewald method with a grid spacing of 1.2 Å and a fourth-order interpolation. The equations of motion were integrated with a time step of 2 fs by the leapfrog algorithm. The simulation duration was 18 ns and the trajectory was saved every 4 ps. Gromacs v4.5.3 package was used for the MD simulation and an in-house code was developed to analyze water flux through the ZIF-8 membrane [48]. Figure S4 shows the number of water molecules passing through the ZIF-8 membrane at 75 °C and 1 bar for 2 wt.% NaCl feed solution.

3. Results and discussions

3.1. Synthesis and characterization of ZIF membranes

In good agreement with our previous report [32], after solvothermal reaction at 85 °C for 24 h, the surface of PDA-modified Al_2O_3 disk is completely covered with a compact ZIF-8 layer, and no cracks, pinholes or other defects are visible in the membrane layer (Fig. 1a). From the cross-section view (Fig. 1b), the ZIF-8 membrane is well intergrown with a thickness of about 20 μm. Attributing to its high covalent reaction ability [32,49], PDA modification is helpful to attract and anchor the ZIF-8 nutrients onto the support surface, thus promoting the nucleation and growth of a dense ZIF-8 layer on the PDA-modified Al_2O_3 disk. The formation of a phase-pure ZIF-8 membrane with a high degree of crystallinity was confirmed by XRD (Fig. 2a), which indicates that all peaks match well with those of ZIF-8 powder besides the α-Al_2O_3 signals from the support [27,32].

3.2. Pervaporation performance of ZIF-8 membrane for seawater desalination

Pervaporation has been widely studied for the separation of organics/water mixtures due to its low energy consumption and ease of operation. Recently, pervaporation is also recommended to be a

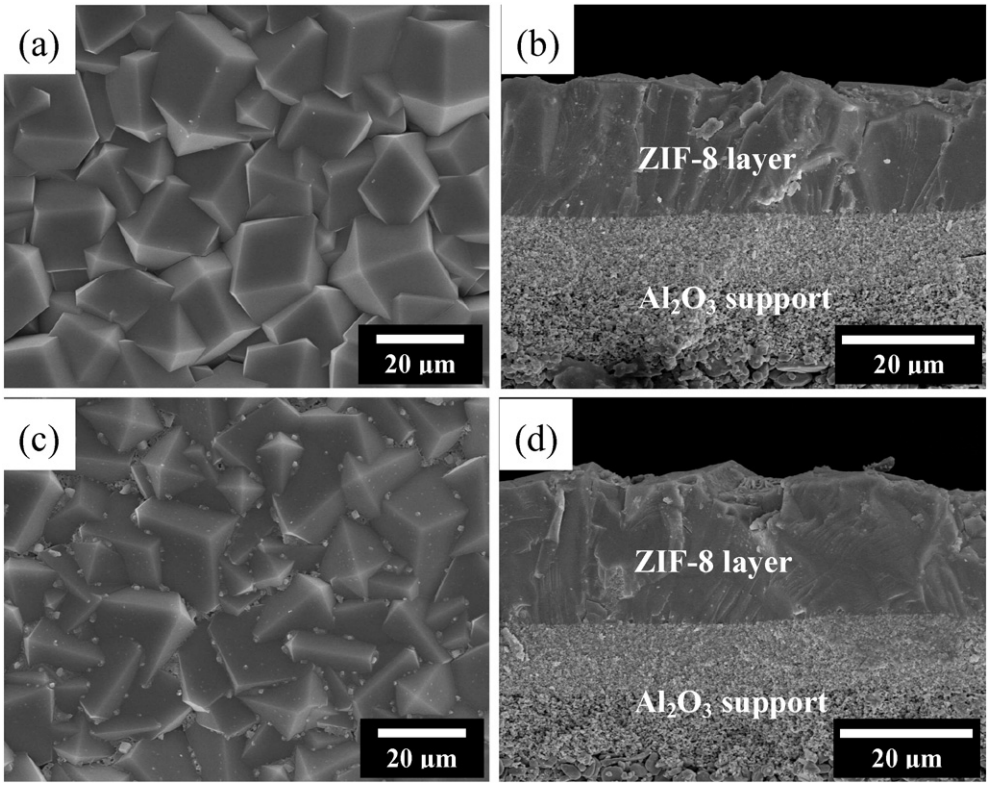

Fig. 1. Top view (a) and cross-section (b) FESEM images of the ZIF-8 membrane used for seawater desalination. Top view (c) and cross-section (d) FESEM images of the ZIF-8 membrane after the measurement of seawater desalination for 24 h at 50 °C through pervaporation.

promising technique for seawater desalination due to its low energy consumption and ease of operation [13,16,17]. The ZIF-8 membrane was sealed in a home-made permeation cell with silicone O-rings and tested for seawater desalination at 25 ~ 100 °C by pervaporation. For the determination of ion rejection, the permeate side of the membrane was washed periodically with de-ionized water to collect possibly permeated salts which have been deposited as crystals on top or inside the porous alumina support, as proposed by previous report [13]. As shown in Fig. 3, at 50 °C, the water flux is 8.1 kg/(m^2·h) and the total ion rejection is over 99.8%, indicating the ZIF-8 membrane displays high separation performance for seawater desalination, even for the ions which are abundantly found in seawater (Table 1). Relative high rejection is also found for Br^- which has a relatively small hydrated diameter, with rejections of 96.5%. In a very recent report [50], the ZIF-8 membrane showed substantial permeation but an unsatisfactory salt rejection due to the presence of inter-crystalline defects.

These results are well consistent with our supposition that the ZIF-8 membrane works following the molecular sieve principle. Since the hydrated ions are excluded from the pore system, water molecules can move easily through the pore system of ZIF-8. These high water fluxes can be understood even “classically” using the solubility-diffusivity concept of membrane permeation. Assuming that the membrane permeability of water can be described as the product of water adsorption and water diffusion in ZIF-8, the low water adsorption is overcompensated by its high diffusivity [51]. Similar results have been observed in Kapteijn's group with DDR membranes. Although that the membrane should be highly hydrophobic, the water flux was pretty high, attributed to a high diffusivity inside the membrane where it is envisaged to have hardly any interaction with the internal surface [52].

The excellent desalination performance of the ZIF-8 membrane is confirmed by a molecular dynamics (MD) simulation (Fig. S3). Fig. 4 shows the simulation snapshots before (at 0 ns) and after a short desalination time (at 18 ns) at 75 °C. It can be seen that more and water molecules can pass through the ZIF-8 membrane in a very short time, while Na^+ or Cl^- ions are excluded by the ZIF-8 membrane. Consequently, seawater desalination can be easily realized by a defect-free ZIF-8 membrane following the ionic sieve principle. This finding is compatible with the MD simulation of salt rejection in reverse osmosis by using zeolite FAU and MFI membranes [53]. Fig. S4 plots the number of water molecules passing through the ZIF-8 membrane at 75 °C and 1 bar for 2 wt.% NaCl feed solution. The water flux is estimated to be 1255.1 kg/(m^2·h) from the MD simulation assuming 6 nm thick ZIF-8 layers and 1 bar pressure difference. When comparing the calculated and measured water permeability, the permeability of the ideal membrane from the MD simulation is approximately 7.5 × 10^{-6} kg·m/(m^2·h·bar), which is lower than the experimental permeability of 216 × 10^{-6} kg·m/(m^2·h·bar). The deviation may be attributed to the presence of inter-crystalline defect and lattice flexibility in the real ZIF-8 membrane, which leads to higher permeability.

When the operation temperature rises from 25 to 100 °C (Fig. 3), the water flux significantly increases from 5.8 to 13.5 kg/(m^2·h), while the ions rejection of the ZIF-8 membrane is almost unchanged. Increase of water flux with increasing temperature is usually observed for microporous membranes in pervaporation process since diffusion increases stronger than adsorption decreases with increasing temperature [54]. Fig. 5 shows an Arrhenius type plot with ln(flux) versus 1/T for water permeation through the ZIF-8 membranes. The linear trend in the plot indicates that water permeation through the ZIF-8 membranes is an activated diffusion process, and the apparent activation energy (E_{act}) is about 10.5 kJ·mol^{-1}, which is comparable to that of water permeation in zeolite membranes [55].

Fig. 6 shows the effect of the feed salt concentration on the water flux and ion rejection of the ZIF-8 membrane. At 50 °C, the water flux decreases from 9.1 to 2.5 kg/(m^2·h) when the feed seawater concentration increases from 2 to 10 wt.%, while the rate of ion rejection still maintains high (99.8%) even for desalination of 10 wt.% seawater. It is usually found that water activity decreases with increasing the salt concentration [16]. In fact, the apparent activation energy (E_{act}) of the

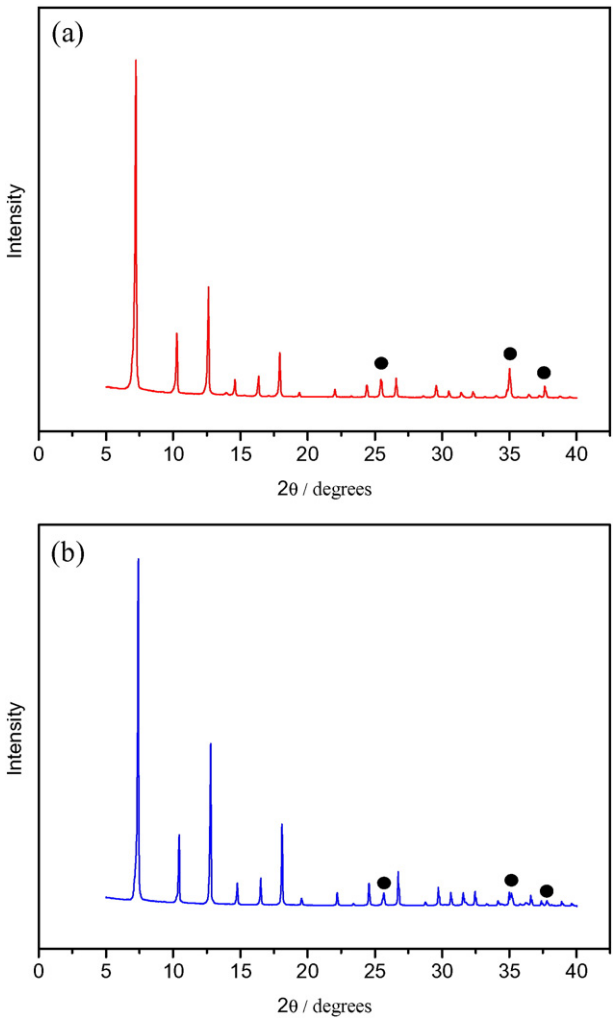

Fig. 2. XRD patterns of the ZIF-8 membrane on Al_2O_3 support before (a) and after (b) the measurement of seawater desalination for 24 h at 50 °C through pervaporation. (●): Al_2O_3 support, (not marked): ZIF-8 crystals.

water permeation for 3.5 wt.% seawater is 10.5 kJ·mol^{-1}, which is lower than that for pure water (12.4 kJ·mol^{-1}, Fig. 7). Therefore, with increasing salt concentration, the driving force for water permeation decreases, thus resulting in the reduction of water flux.

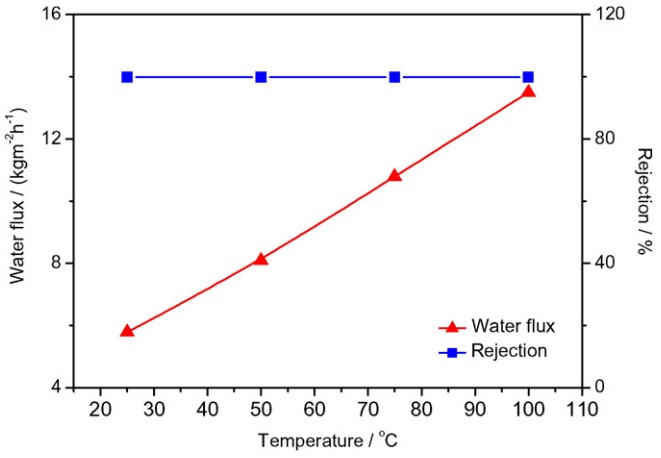

Fig. 3. Water flux and ion rejection of the ZIF-8 membrane as a function of the operation temperature for seawater desalination by pervaporation for 24 h.

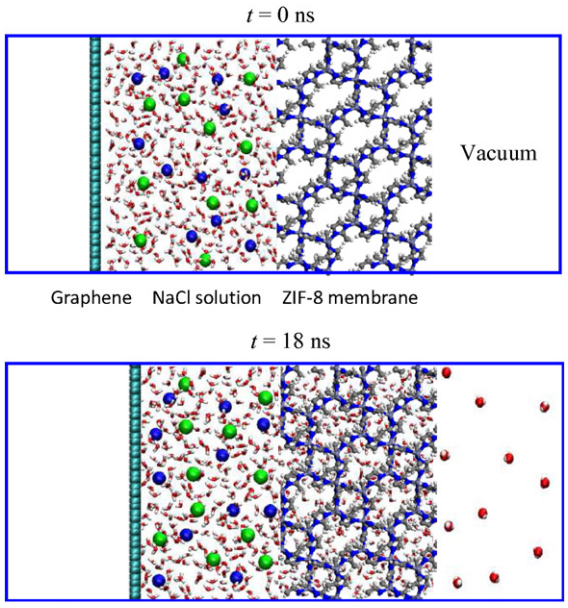

Fig. 4. Simulation snapshots at t = 0 and 18 ns at 75 °C. Color code: Na^+, blue sphere; Cl^-, green sphere; H, white; O, red. An impermeable graphene plate is used to seal the feed side from the surrounding.

In addition to the ZIF-8 membrane, other ZIF membranes such as ZIF-7 and ZIF-90 can also be facilely formed on the PDA-modified Al_2O_3 disks and are effective for seawater desalination. High water flux and high salt rejection (over 99.5%) is consistently observed for both ZIF-7 and ZIF-90 membranes (Fig. S5, S6). Similar to the ZIF-8 membrane, with increasing the temperature from 25 to 100 °C, the water flux increases continuously, while the salt rejection keeps almost unchanged. It is worth noted that the synthesis of ZIF-8 is much easier and cheaper than the synthesis of ZIF-7 and ZIF-90, which is helpful to prepare the ZIF-8 membrane in large-scale.

Membrane-based desalination is one of the most promising technologies for producing fresh water from seawater due to its low energy consumption. It is well recognized that the membrane materials play an important role in determining the water productivity and energy costs. Inorganic zeolite membranes have drawn much interest for seawater desalination due to their high stability and uniform pore structure. Comparing with the literature data of seawater desalination on microporous zeolite membranes as well as other RO membranes (Table S1), the ZIF membranes developed in this work demonstrate

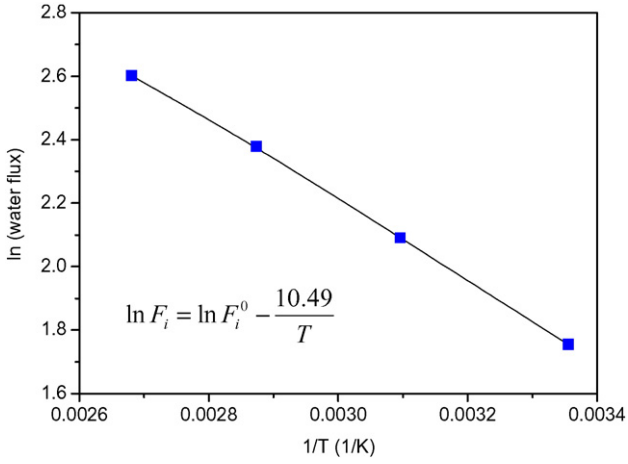

Fig. 5. Variation of ln(water flux) versus 1/T through the ZIF-8 membrane for pervaporation of 3.5 wt.% seawater.

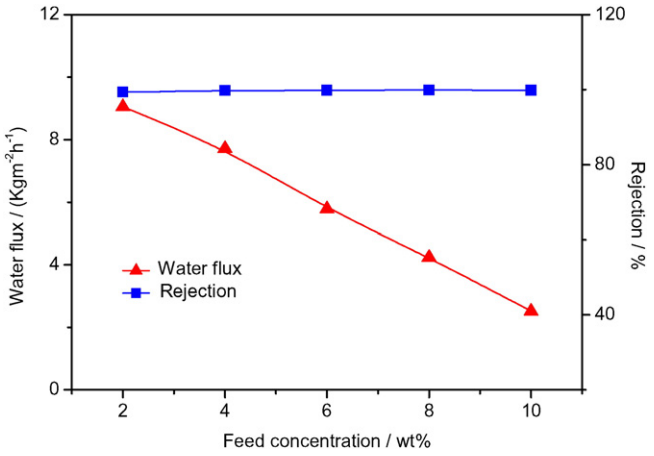

Fig. 6. Water flux and ion rejection of the ZIF-8 membrane by pervaporation as function of the feed seawater concentration at 50 °C.

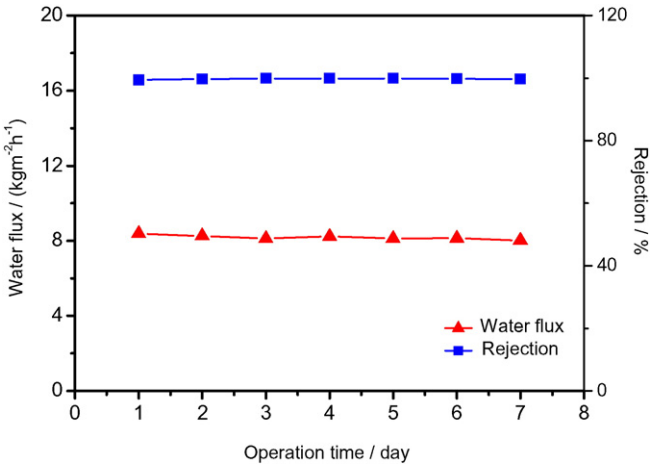

Fig. 8. Stability measurement of the ZIF-8 membrane for desalination of 3.5 wt.% seawater by pervaporation at 50 °C.

very high water flux and ion rejection. Further, since PDA modification of the supports can enhance the reproducibility of membrane preparation [32], a high ion rejection is found in three independently prepared and tested ZIF-8 membranes (Table S2).

3.3. Stability evaluation of the ZIF-8 membrane for seawater desalination

The studied on the stability of ZIF-8 in the aqueous solution have drawn increasing interest. Yaghi and co-workers reported no change in crystallinity and porosity of ZIF-8 crystals after being placed in boiling water for as long as 7 days [27]. Lai and co-workers reported the successful synthesis of ZIF-8 crystals in pure aqueous solution [56]. However, Lin and co-workers reported that ZIF-8 crystals will be degraded in water, but he rate and extent of the dissolution depends on the ZIF-8 crystal to water mass ratio [57]. Similar result was also reported by Yang and co-workers [58]. It was reported that ZIF-8 crystals are ready to hydrolyze under hydrothermal conditions when contact with water at lower weight ratio of ZIF crystals to water (0.06 wt.%). In some recent reviews by Canivet and Burtch, the limits and promises of the MOF stability towards water are treated [59,60]. In a previous pioneering paper by Low, a good overview on the steam stability of MOFs as a function of temperature is given [61]. Anyway, all the pioneering reports suggest that ZIF-8 belongs to one of the most stable MOF structures. Therefore, it is necessary to evaluate the stability of the ZIF-8 membrane for seawater desalination.

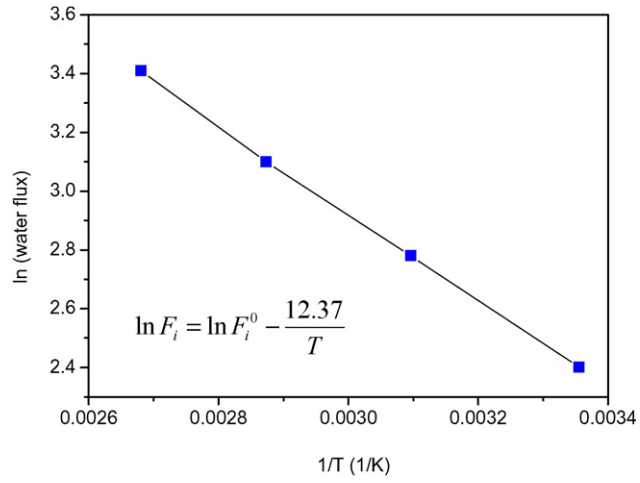

Fig. 7. Variation of ln(water flux) versus 1/T through the ZIF-8 membrane for pervaporation of pure water.

As shown in Fig. 1c and d, after the measurement of seawater desalination at 50 °C for 24 h, there are no remarkable differences in membrane morphology besides a few loose seawater salt crystals deposited on membrane surface (when removing the membrane without further washing), and the ZIF-8 membrane is still well intergrown without any visible cracks, pinholes or other defects. A typical XRD pattern (Fig. 2b) shows that the high crystallinity of the ZIF-8 membrane remains unchanged after the measurement of seawater desalination. All the XRD peaks of the ZIF-8 membrane match well with those of the as-prepared ZIF-8 membrane, indicating that the unusual thermal and chemical stability of ZIF-8 allows it being used for seawater desalination under relative harsh conditions. Further, from the cross-section EDXS pattern of the ZIF-8 membrane (Fig. S7) and XPS of the permeate side of the ZIF-8 membrane (Fig. S8) after the measurement of seawater desalination, only a few ions can be observed in the membrane layer and almost no ions can be detected in the permeate side, suggesting the ions are effectively excluded to pass through the ZIF-8 membrane.

Fig. 8 shows the separation performance of the ZIF-8 membrane which was evaluated for seawater desalination for 7 days at 50 °C. It can be seen that the salt rejection is almost constant whereas the water flux shows only slight reduction, indicating that the ZIF-8 membrane has a high stability in seawater desalination. In complete accordance with the constant water flux and salt rejection, no notable

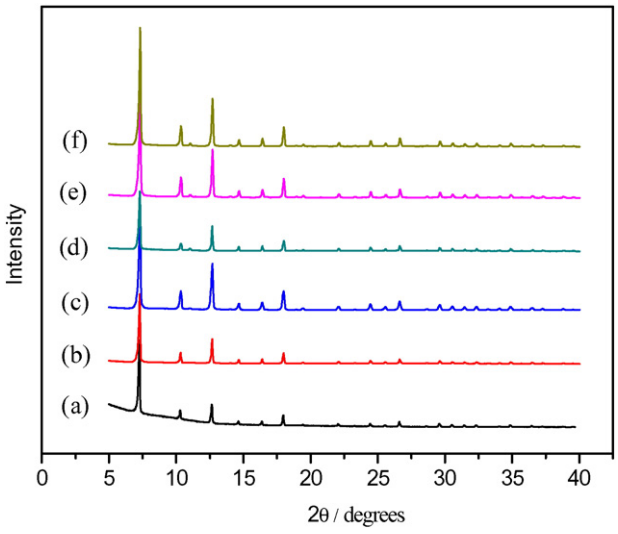

Fig. 9. XRD patterns of the ZIF-8 crystals which was treated by 3.5 wt.% seawater at 20 °C for 1 day (a), 2 days (b), 4 days (c), 8 days (d), 10 days (e), and 15 days (f).

changes in XRD pattern of the ZIF-8 can be observed after 15 days treatment with 3.5 wt.% seawater (Fig. 9), further confirming the high stability of ZIF-8 in contact with seawater.

4. Conclusion

In conclusion, in the present work we have successfully developed stable ZIF membranes for seawater desalination. Attributing to the small aperture size as well as the high stability in seawater, the developed ZIF membranes display high separation performances for seawater desalination as demonstrated by both experimental and simulation studies. At 25, 50, 75 and 100 °C, the water fluxes through the ZIF-8 membrane are 5.8, 8.1, 10.8, and 13.5 kg/(m^2·h), respectively, with ion rejections of over 99.8%, which are superior to conventional zeolite membranes. This high separation performances combined with high stability suggest that the developed ZIF membranes are promising candidates for seawater desalination by ionic sieving.

Acknowledgments

This work is supported by the National Natural Science Foundation of China (51402320), External Cooperation Program of BIC, Chinese Academy of Science (174433KYSB2013005), Ningbo Science and Technology Innovation Team (2014B81004), Ningbo Municipal Natural Science Foundation (2015A610046), and A*star of Singapore (R-279-000-431-305).

Appendix A. Supplementary data

Supplementary data to this article can be found online at http://dx.doi.org/10.1016/j.desal.2016.02.005.

References

[1] R. F. Service, Desalination freshens up, Science 311 (2006) 1088–1090.
[2] M.A. Shannon, P.W. Bohn, M. Elimelech, J.G. Georgiadis, B.J. Mariñas, A.M. Mayes, Science and technology for water purification in the coming decades, Nature 452 (2008) 301–310.
[3] Q. Schiermeier, Purification with a pinch of salt, Nature 452 (2008) 260–261.
[4] M. Elimelech, W.A. Phillip, The future of seawater desalination: energy, technology, and the environment, Science 333 (2011) 712–717.
[5] M.G. Marcovecchio, S.F. Mussati, P.A. Aguirre, N.J. Scenna, Optimization of hybrid desalination processes including multi stage flash and reverse osmosis systems, Desalination 182 (2005) 111–122.
[6] A.D. Khawaji, I.K. Kutubkhanah, J.-M. Wie, Advances in seawater desalination technologies, Desalination 221 (2008) 47–69.
[7] W. Zhu, L. Gora, A.W.C. van den Berg, F. Kapteijn, J.C. Jansen, J.A. Moulijn, Water vapour separation from permanent gases by a zeolite-4A membrane, J. Membr. Sci. 253 (2005) 57–66.
[8] J. Glater, S.K. Hong, M. Elimelech, The search for a chloring-resistant reverse-osmosis membrane, Desalination 95 (1994) 325–345.
[9] H. El-Saied, A.H. Basta, B.N. Barsoum, M.M. Elberry, Cellulose membranes for reverse osmosis part I. RO cellulose acetate membranes including a composite with polypropylene, Desalination 159 (2003) 171–181.
[10] L. Li, J. Dong, T.M. Nenof, R. Lee, Desalination by reverse osmosis using MFI zeolite membranes, J. Membr. Sci. 243 (2004) 401–404.
[11] L. Li, N. Liu, B. McPherson, R. Lee, Influence of counter ions on the reverse osmosis through MFI zeolite membranes: implications for produced water desalination, Desalination 228 (2008) 217–225.
[12] L. Li, N. Liu, B. McPherson, R. Lee, Enhanced water permeation of reverse osmosis through MFI-type zeolite membranes with high aluminum contents, Ind. Eng. Chem. Res. 46 (2007) 1584–1589.
[13] M.C. Duke, J. O'Brien-Abraham, N. Milne, B. Zhu, Jerry Y.S. Lin, J.C. Diniz da Costa, Seawater desalination performance of MFI type membranes made by secondary growth, Sep. Purif. Technol. 68 (2009) 343–350.
[14] Z. Zhu, N. Hong, C. Milne, M. Doherty, L. Zou, Y.S. Lin, A.J. Hill, X. Gu, M. Duke, Desalination of seawater ion complexes by MFI-type zeolite membranes: temperature and long term stability, J. Membr. Sci. 453 (2014) 12–135.
[15] R. Covarrubias, R. Garcia, J. Arriagada, H. Yanez, Z. Ramanan, M. Lai, Tsapatsis, removal of trivalent chromium contaminant from aqueous media using FAU-type zeolite membranes, J. Membr. Sci. 312 (2008) 163–173.
[16] C.H. Cho, K.Y. Oh, S.K. Kim, J.G. Yeo, P. Sharma, Pervaporative seawater desalination using NaA zeolite membrane: mechanisms of high water flux and high salt rejection, J. Membr. Sci. 371 (2011) 226–238.
[17] S. Khajavi, J.C. Jansen, F. Kapteijn, Production of ultra pure water by desalination of seawater using a hydroxy sodalite membrane, J. Membr. Sci. 356 (2010) 52–57.
[18] C. Jiang, Q. Wang, Y. Zhang, Y. Li, Y. Wang, T. Xu, Separation of methionine from the mixture with sodium carbonate using bipolar membrane electrodialysis, J. Membr. Sci. 498 (2016) 48–56.
[19] C.P. Athanasekou, N.G. Moustakas, S. Morales-Torres, L.M. Pastrana-Martínez, J.L. Figueiredo, J.L. Faria, A.M.T. Silva, J.M. Dona-Rodriguez, G. Em.Romanos, P. Falaras, Ceramic photocatalytic membranes for water filtration under UV and visible light, Appl. Catal. B Environ. 178 (2015) 12–19.
[20] Y.S. Dzyazko, A.S. Rudenko, Y.M. Yukhin, A.V. Palchik, V.N. Belyakov, Modification of ceramic membranes with inorganic sorbents. Application to electrodialytic recovery of Cr(VI) anions from multicomponent solution, Desalination 342 (2014) 52–60.
[21] J. Kuhn, S. Sutanto, J. Gascon, J. Gross, F. Kapteijn, Performance and stability of multichannel MFI zeolite membranes detemplated by calcination and ozonication in ethanol/water pervaporation, J. Membr. Sci. 339 (2009) 261–274.
[22] J.A. Stoeger, J. Choi, M. Tsapatsis, Rapid thermal processing and separation performance of columnar MFI membranes on porous stainless steel tubes, Energ. Environ. Sci. 4 (2011) 3479–3486.
[23] Bétard, R.A. Fischer, Metal–organic framework thin films: from fundamentals to applications, Chem. Rev. 112 (2012) 1055–1083.
[24] R. Ranjan, M. Tsapatsis, Microporous metal organic framework membrane on porous support using the seeded growth method, Chem. Mater. 21 (2009) 4920–4924.
[25] H. Guo, G. Zhu, I.J. Hewitt, S. Qiu, "Twin copper source" growth of metal–organic framework membrane: $Cu_3(BTC)_2$ with high permeability and selectivity for recycling H_2, J. Am. Chem. Soc. 131 (2009) 1646–1647.
[26] J. Gascon, F. Kapteijn, Metal–organic framework membranes-high potential, bright future? Angew. Chem. Int. Ed. 49 (2010) 1530–1532.
[27] K.S. Park, Z. Ni, A.P. Côté, J.Y. Choi, R. Huang, F.J. Uribe-Romo, H.K. Chae, M. O'Keeffe, O.M. Yaghi, Exceptional chemical and thermal stability of zeolitic imidazolate frameworks, Proc. Natl. Acad. Sci. U. S. A. 103 (2006) 10186–10191.
[28] J.J. Low, A.I. Benin, P. Jakubczak, J.F. Abrahamian, S.A. Faheem, R.R. Willis, Virtual high throughput screening confirmed experimentally: porous coordination polymer hydration, J. Am. Chem. Soc. 131 (2009) 15834–15842.
[29] Y. Li, F. Liang, H. Bux, A. Feldhoff, W. Yang, J. Caro, Molecular sieve membrane: supported metal–organic framework with high hydrogen selectivity, Angew. Chem. Int. Ed. 49 (2010) 548–551.
[30] Z. Xie, J. Yang, J. Wang, J. Bai, H. Yin, B. Yuan, J. Lu, Y. Zhang, L. Zhou, C. Duan, Deposition of chemically modified α-Al_2O_3 particles for high performance ZIF-8 membrane on a macroporous tube, Chem. Commun. 48 (2012) 5977–5979.
[21] H. Bux, F. Liang, Y. Li, J. Cravillon, M. Wiebcke, J. Caro, Zeolitic imidazolate framework membrane with molecular sieving properties by microwave-assisted solvothermal synthesis, J. Am. Chem. Soc. 131 (2009) 16000–16001.
[32] Q. Liu, N. Wang, J. Caro, A. Huang, Bio-inspired polydopamine: a versatile and powerful platform for covalent synthesis of molecular sieve membranes, J. Am. Chem. Soc. 135 (2013) 17679–17682.
[33] H.T. Kwon, H.-K. Jeong, In situ synthesis of thin zeolitic-imidazolate framework ZIF-8 membranes exhibiting exceptionally high propylene/propane separation, J. Am. Chem. Soc. 135 (2013) 10763–10768.
[34] A. Huang, H. Bux, F. Steinbach, J. Caro, Molecular-sieve membrane with hydrogen permselectivity: ZIF-22 in LTA topology prepared with 3-aminopropyltriethoxysilane as covalent linker, Angew. Chem. Int. Ed. 49 (2010) 4958–4961.
[35] Y. Liu, G. Zeng, Y. Pan, Z. Lai, Synthesis of highly c-oriented ZIF-69 membranes by secondary growth and their gas permeation properties, J. Membr. Sci. 379 (2011) 46–51.
[36] X. Dong, Y.S. Lin, Synthesis of an organophilic ZIF-71 membrane for pervaporation solvent separation, Chem. Commun. 49 (2013) 1196–1198.
[37] A. Huang, W. Dou, J. Caro, Steam-stable zeolitic imidazolate framework ZIF-90 membrane with hydrogen selectivity through covalent functionalization, J. Am. Chem. Soc. 132 (2010) 15562–15564.
[38] A. Huang, N. Wang, C. Kong, J. Caro, Organosilica-functionalized zeolitic imidazolate framework ZIF-90 membrane with high gas separation performance, Angew. Chem. Int. Ed. 51 (2012) 10551–10555.
[39] J. Brown, R. Johnson, M.E. Lydon, W.J. Koros, C.W. Jone, S. Nair, Continuous polycrystalline zeolitic imidazolate framework-90 membranes on polymeric hollow fibers, Angew. Chem. Int. Ed. 251 (2012) 10615–10618.
[40] A. Huang, Y. Chen, N. Wang, Z. Hu, J. Jiang, J. Caro, A highly permeable and selective zeolitic imidazolate framework ZIF-95 membrane for H_2/CO_2 separation, Chem. Commun. 48 (2012) 10981–10983.
[41] A.K. Rappé, C.J. Casewit, K.S. Colwell, W.A. Goddard Iii, W.M. Skiff, UFF, a full periodic table force field for molecular mechanics and molecular dynamics simulations, J. Am. Chem. Soc. 114 (1992) 10024–10035.
[42] Z. Hu, Y. Chen, J. Jiang, Zeolitic imidazolate framework-8 as a reverse osmosis membrane for water desalination: insight from molecular simulation, J. Chem. Phys. 134 (2011) 134705.
[43] W.L. Jorgensen, J. Chandrasekhar, J.D. Madura, R.W. Impey, M.L. Klein, Comparison of simple potential functions for simulating liquid water, J. Chem. Phys. 79 (1983) 926–935.
[44] W.D. Cornell, P. Cieplak, C.I. Bayly, I.R. Gould, K.M. Merz, D.M. Ferguson, P.A. Kollman, A second generation force field for the simulation of proteins, nucleic acids, and organic molecules, J. Am. Chem. Soc. 117 (1995) 5179–5197.
[45] G. Hummer, J.C. Rasaiah, J.P. Noworyta, Water conduction through the hydrophobic channel of a carbon nanotube, Nature 414 (2001) 188–190.
[46] S. Miyamoto, P.A. Kollman, SETTLE: an analytical version of the SHAKE and RATTLE algorithm for rigid water models, J. Comput. Chem. 13 (1992) 952–962.

[47] G. Bussi, D. Donadio, M. Parrinello, Canonical sampling through velocity rescaling, J. Chem. Phys. 126 (2007) 014101.
[48] D. Van Der Spoel, E. Lindahl, B. Hess, G. Groenhof, A.E. Mark, H.J. Berendsen, GROMACS: fast, flexible, and free, J. Comput. Chem. 26 (2005) 1701–1718.
[49] H. Lee, S.M. Dellatore, W.M. Miller, P.B. Messersmith, Mussel-inspired surface chemistry for multifunctional coatings, Science 318 (2007) 426–430.
[50] M.C. Duke, B. Zhu, C.M. Doherty, M.R. Hill, A.J. Hill, M.A. Carreon, Structural effects on SAPO-34 and ZIF-8 materials exposed to seawater, solutions, and their potential as desalination membranes, Desalination 377 (2016) 128–137.
[51] K. Zhang, R.P. Lively, C. Zhang, R.R. Chance, W.J. Koros, D.S. Sholl, S. Nair, Exploring the framework hydrophobicity and flexibility of ZIF-8: from biofuel recovery to hydrocarbon separations, J. Phys. Chem. Lett. 4 (2013) 3618–3622.
[52] J. Kuhn, K. Yajima, T. Tomita, J. Gross, F.J. Kapteijn, Dehydration performance of a hydrophobic DD3R zeolite membrane, J. Membr. Sci. 321 (2008) 344–349.
[53] Y. Liu, X. Chen, High permeability and salt rejection reverse osmosis by a zeolite nano-membrane, Phys. Chem. Chem. Phys. 15 (2013) 6817–6824.
[54] D. Shah, K. Kissick, A. Ghorpade, R. Hannah, D.J. Bhattacharyy, Pervaporation of alcohol–water and dimethylformamide–water mixtures using hydrophilic zeolite NaA membranes: mechanisms and experimental results, J. Membr. Sci. 179 (2010) 185–205.
[55] B. Huang, Q. Liu, J. Caro, A. Huang, Iso-butanol dehydration by pervaporation using zeolite LTA membranes prepared on 3-aminopropyltriethoxysilane-modified alumina tubes, J. Membr. Sci. 455 (2014) 200–206.
[56] Y. Pan, Y. Liu, G. Zeng, L. Zhao, Z. Lai, Rapid synthesis of zeolitic imidazolate framework-8 (ZIF-8) nanocrystals in an aqueous system, Chem. Commun. 47 (2011) 2071–2073.
[57] H. Zhang, D. Liu, Y. Yao, B. Zhang, Y.S. Lin, Stability of ZIF-8 membranes and crystalline powders in water at room temperature, J. Membr. Sci. 485 (2015) 103–111.
[58] X.L. Liu, Y.S. Li, Y.J. Ban, Y. Peng, H. Jin, H. Bux, L.Y. Xu, J. Caro, W.S. Yang, Improvement of hydrothermal stability of zeolitic imidazolate frameworks, Chem. Commun. 49 (2013) 9140–9142.
[59] J. Canivet, A. Fateeva, Y. Guo, B. Coasne, D. Farusseng, Water adsorption in MOFs: fundamentals and applications, Chem. Soc. Rev. 43 (2014) 5594–5617.
[60] N.C. Burtch, H. Jasuja, K.S. Walton, Water stability and adsorption in metal–organic frameworks, Chem. Rev. 114 (2014) 10575–10612.
[61] J.J. Low, A.I. Benin, P. Jakubczak, J.F. Abrahamian, S.A. Faheem, R.R. Willis, Virtual high throughput screening confirmed experimentally: porous coordination polymer hydration, J. Am. Chem. Soc. 131 (2009) 15834–15842.